

Environment and properties of emitting electrons in blazar jets: Mrk 421 as a laboratory

Nijil Mankuzhiyil

INFN Trieste and Università di Udine, via delle Scienze 208, I-33100 Udine, ITALY

Stefano Ansoldi

International Center for Relativistic Astrophysics (ICRA), Rome and Università di Udine, via delle Scienze 208, I-33100 Udine, ITALY

Massimo Persic

INAF-Trieste, via G. B. Tiepolo 11, I-34143 Trieste, ITALY

Fabrizio Tavecchio

INAF-Brera, via E. Bianchi 46, I-23807 Merate, ITALY

Here we report our recent study on the spectral energy distribution (SED) of the high frequency BL Lac object Mrk 421 in different luminosity states. We used a full-fledged χ^2 -minimization procedure instead of more commonly used "eyeball" fit to model the observed flux of the source (from optical to very high energy), with a Synchrotron-Self-Compton (SSC) emission mechanism. Our study shows that the synchrotron power and peak frequency remain constant with varying source activity, and the magnetic field (B) decreases with the source activity while the break energy of electron spectrum (γ_{br}) and the Doppler factor (δ) increase. Since a lower magnetic field and higher density of electrons result in increased electron-photon scattering efficiency, the Compton power increases, so does the total emission.

1. Introduction

Active galactic nuclei (AGN) involve the most powerful, steady sources of luminosity in the Universe. It is believed that the center core of AGN consist of super massive black hole (SMBH) surrounded by an accretion disk. In some cases powerful collimated jets are found in AGN, perpendicular to the plane of accretion disk. The origin of jets are still unclear. AGNs whose jets are viewed at a small angle to its axis are called blazars.

The overall (radio to γ -ray) spectral energy distribution (SED) of blazars shows two broad non-thermal continuum peaks. The low-energy peak is thought to arise from electron synchrotron emission. The leptonic model suggests that the second peak forms due to inverse Compton emission. This can be due to upscattering, by the same non-thermal population of electrons responsible for the synchrotron radiation, and synchrotron photons (Synchrotron Self Compton: SSC) Maraschi et al. [1992].

Blazars often show violent flux variability, that may or may not appear correlated in the different energy bands. Simultaneous observation are then crucial to understand the physics behind variability.

2. χ^2 -minimized SED fitting

In this section we discuss the code that we have used to obtain an estimation of the characteristic parameters of the SSC model. The SSC model assumes a spectrum for the accelerated electron density k , which is a broken power law with exponents n_1 and n_2 . The minimum, maximum and break Lorentz factors for the

```

DEF: SSC parameters initial values set-up
calculate initial  $\chi^2$  value, change parameters
LOOP :
  calculate  $\chi^2$  for modified parameters
  if  $\chi^2$  has increased:
    we are moving away from a minimum
     $\Rightarrow$  change parameters, increase weight
      of steepest descent method and reset
      negligible decrease amount counter
  if  $\chi^2$  has decreased:
    we are moving toward a minimum
     $\Rightarrow$  change parameters and increase
      weight of inverse Hessian method
UNTIL:  $\chi^2$  decreases by a negligible amount
for the fourth time

```

Table I The χ^2 minimization algorithm.

electrons are usually called γ_{min} , γ_{max} . and γ_{break} respectively. The emitting region is considered to be a blob of radius R moving with Doppler factor δ with respect to the observer in a magnetic field of intensity B . The model is thus characterized by nine free parameters.

In the present work we have kept γ_{min} . fixed and equal to unit, which is a satisfactory approximation already used in the literature. The determination of the remaining eight parameters has been performed by finding their best values and uncertainties from a χ^2 minimization in which multi-frequency experi-

mental points have been fitted to the SSC spectrum modelled as in Tavecchio et al. [1998]. Minimization has been performed using the Levenberg-Marquardt method Press et al. [1994], which is an efficient standard for non-linear least-squares minimization that smoothly interpolates between two different minimization approaches, namely the inverse Hessian method and the steepest descent method. For completeness, we briefly present the pseudo-code for the algorithm in table I.

A crucial point in our implementation is that from Tavecchio et al. [1998] we can only obtain a numerical approximation to the SSC spectrum, in the form of a sampled SED. On the other hand, from table I, we understand that at each step the calculation of the χ^2 requires the evaluation of the SED for all the observed frequencies. Although an observed point will likely not be one of the sampled points coming from Tavecchio et al. [1998], it will fall between two sampled points, so that interpolation can be used to approximate the value of the SED¹.

At the same time, the Levenberg-Marquardt method requires the calculation of the partial derivatives of χ^2 with respect to the SSC parameters. These derivatives have also been obtained numerically by evaluating the incremental ratio of the χ^2 with respect to a sufficiently small, dynamically adjusted increment of each parameter. This method could have introduced a potential inefficiency in the computation, due to the recurrent need to evaluate the SED at many, slightly different points in parameter space, this being the most demanding operation in terms of CPU time. For this reason we set up the algorithm to minimize the number of calls to Tavecchio et al. [1998] across different iterations. The χ^2 fit during different iterations are shown in Fig. 1.

3. Application and results

In order to study the behavior of parameters with source activity, we choose Mrk 421 (table II), considering the larger availability of MWL data sets and the lower redshift, hence less uncertainty after EBL correction of VHE data. The χ^2 fitted SEDs are shown in Fig. 2.

In addition to the χ^2 test, we also checked the goodness of the fit using the Kolmogorov-Smirnov (KS) test. Considering the occurrence of different physical processes (synchrotron and inverse Compton, at substantially different energies), and the different quality

Table II Data sets used in this study. The observation period of each state can be found at Fig. 2.

State	Instruments	References
1.	XMM-Newton Whipple, MAGIC	Acciari et al. [2009]
2.	XMM-Newton Whipple, MAGIC	Acciari et al. [2009]
3.	KVA, WIYN, RXTE Whipple, HEGRA-CT 1	Rebillot et al. [2006]
4.	Boltwood, RXTE Whipple	Blazejewski et al. [2005]
5.	Havard-Smithsonian RXTE, Whipple	Fossati et al. [2008]
6.	XMM-Newton VERITAS	Acciari et al. [2009]
7.	Havard-Smithsonian RXTE, Whipple	Fossati et al. [2008]
8.	WEBT, <i>Swift</i> RXTE, VERITAS	Donnarumma et al. [2009]
9.	Boltwood, RXTE Whipple	Blazejewski et al. [2005]

of low- and high-energy data, we used a *piecewise KS test*, i.e. we applied the KS test separately to low- and high-energy data. Then the KS test always confirms that the fit residuals are normal at 5% confidence level.

Our results suggest that in Mkn 421, B decreases with source activity whereas γ_{break} and δ increase (Fig. 3 top). This can be interpreted in a frame where the synchrotron power and peak frequency remain constant with varying source activity by decreasing magnetic field and increasing the number of low energy electrons. This mechanism results in an increased electron-photon scattering efficiency and hence in an increased Compton power. Other emission parameters appear uncorrelated with source activity. In Fig. 3 (bottom), the B - γ_{break} anti-correlation results from a roughly constant synchrotron peak frequency. The B - δ correlation suggests that the Compton emission of Mkn 421 is always in the Thomson limit. The δ - γ_{break} correlation is an effect of the constant synchrotron and Compton frequencies of the radiation emitted by a plasma in bulk relativistic motion towards the observer.

More detailed description of this work is available in Mankuzhiyil et al. [2011].

¹The sampling of the SED function coming from Tavecchio et al. [1998] is dense enough, so that, with respect to other uncertainties, the one coming from this interpolation is negligible.

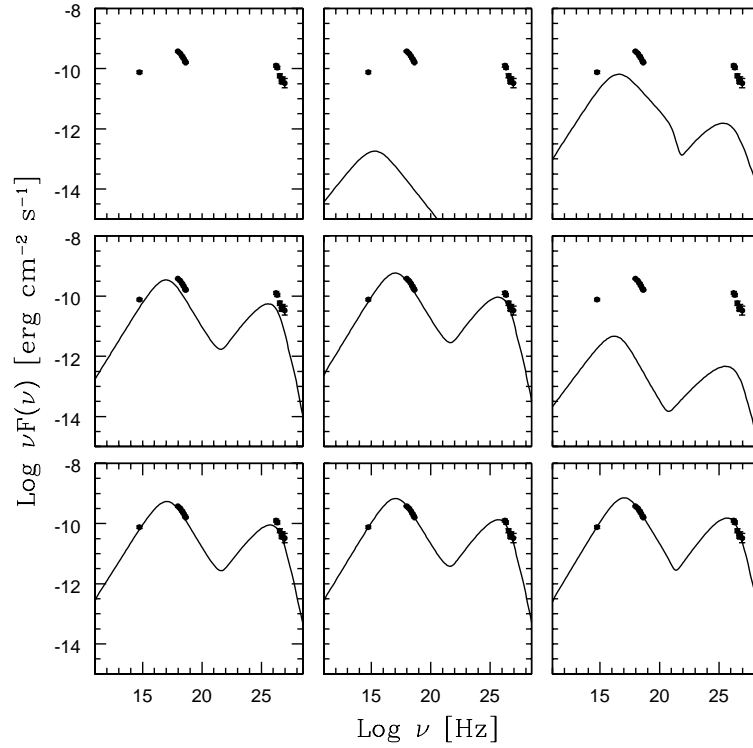


Figure 1: Steps during χ^2 minimization iterations.

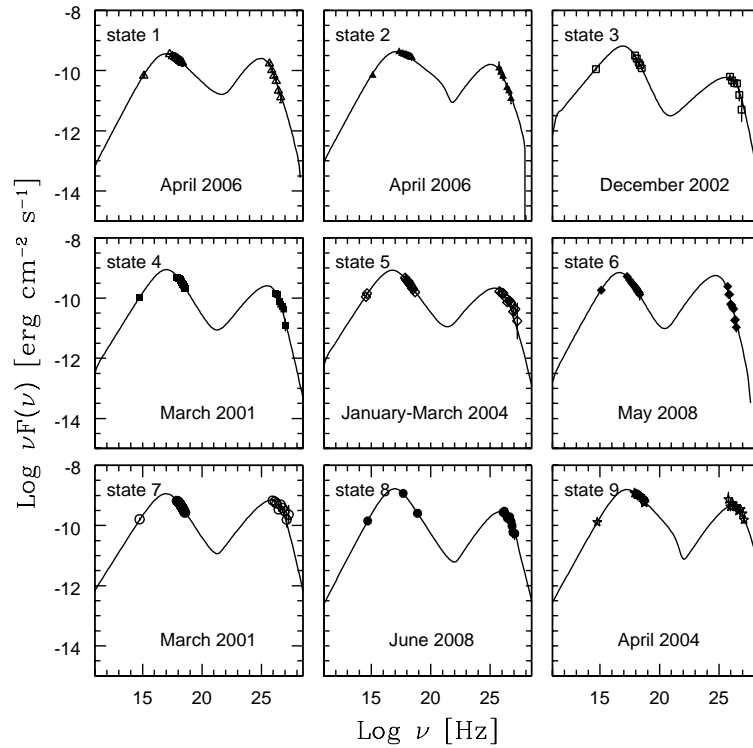


Figure 2: Mrk 421 MWL data sets and corresponding χ^2 minimized SED fits.

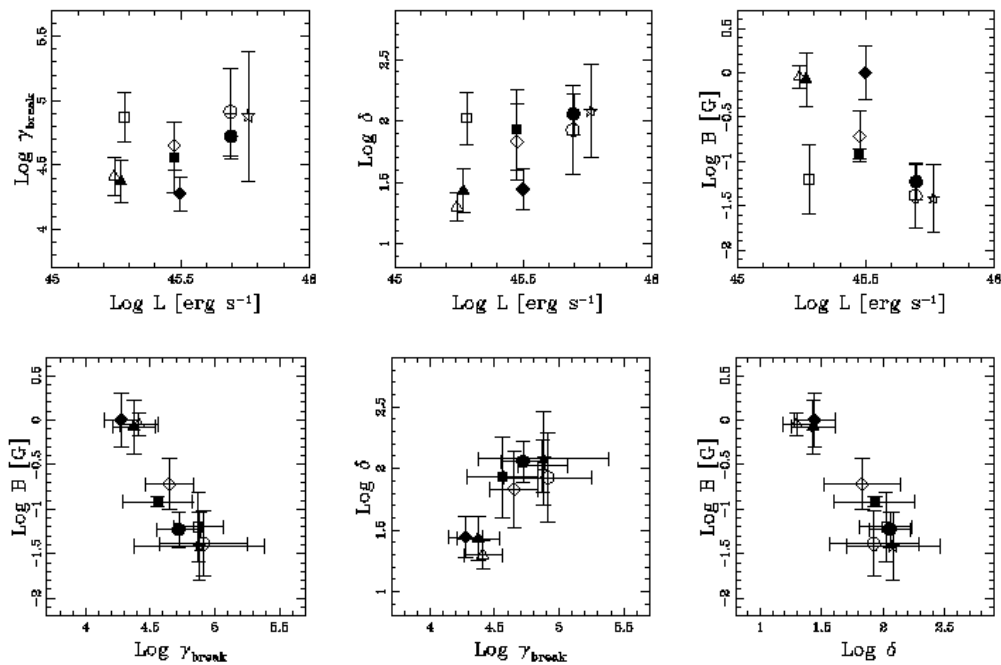


Figure 3: *Top.* Variations of the fitted parameters - B , δ , and γ_{br} - as a function of luminosity. The other SSC parameters show a scatter plot with the luminosity. Parameters and its uncertainty can be found at Mankuzhiyil et al. [2011]. *Bottom.* Correlations between B , δ , and γ_{br} .

References

- Acciari, V. A., et al. (VERITAS Collaboration) 2009, ApJ, 703, 169
 Blazejowski M. et al. 2005, ApJ, 630, 130
 Donnarumma I. et al. 2009, ApJ, 691, L13
 Fossati, G., Buckley, J.H., Bond, I.H., et al. 2008, ApJ, 677, 906
 Mankuzhiyil, N., Ansoldi, S., Persic, M., Tavecchio, F. 2011, ApJ, 733, 14
 Maraschi, L., Ghisellini, G., & Celotti, A. 1992, ApJ, 397, L5
 Press, W.H., et al. 1992, Numerical Recipes (Cambridge: Cambridge University Press)
 Rebillot, P. et al. 2006, ApJ, 641, 740
 Tavecchio, F., Maraschi, L., & Ghisellini, G. 1998, ApJ, 509, 608 (T98)